ACS OMEGA

Cite This: ACS Omega 2019, 4, 12782−12789

Article

http://pubs.acs.org/journal/acsodf

Evaluation of Synthetic Cytochrome P_{450}-Mimetic Metalloporphyrins To Facilitate "Biomimetic" Biotransformation of a Series of $mGlu_5$ Allosteric Ligands

Christopher C. Presley,[†] Charles K. Perry,[†] Elizabeth S. Childress,[†] Matthew J. Mulder,[†] Vincent B. Luscombe,[†] Alice L. Rodriguez,[†] Colleen M. Niswender,[†,Φ,€,¥] P. Jeffrey Conn,[†,Φ,€,¥] and Craig W. Lindsley*[,†,Φ,γ,ψ,¥]

[†]Vanderbilt Center for Neuroscience Drug Discovery, [Φ]Department of Pharmacology, [γ]Department of Biochemistry, and [€]Vanderbilt Kennedy Center, Vanderbilt University School of Medicine, Nashville, Tennessee 37232, United States

[ψ]Department of Chemistry and [¥]Vanderbilt Institute of Chemical Biology, Vanderbilt University, Nashville, Tennessee 37232, United States

Supporting Information

ABSTRACT: Allosteric ligands within a given chemotype can have the propensity to display a wide range of pharmacology, as well as unexpected changes in GPCR subtype selectivity, typically mediated by single-atom modifications to the ligand. Due to the unexpected nature of these "molecular switches", chemotypes with this property are typically abandoned in lead optimization. Recently, we have found that in vivo oxidative metabolism by CYP_{450}s can also engender molecular switches within allosteric ligands, changing the mode of pharmacology and leading to unwanted toxicity. We required a higher-throughput approach to assess in vivo metabolic molecular switches, and we turned to a "synthetic liver", a 96 well kit of biomimetic catalysts (e.g., metalloporphyrins) to rapidly survey a broad panel of synthetic CYP_{450}s' ability to oxidize/"metabolize" an $mGlu_5$ PAM (VU0403602) known to undergo an in vivo CYP_{450}-mediated molecular switch. While the synthetic CYP_{450}s did generate a number of oxidative "metabolites" at known "hot spots", several of which proved to be pure $mGlu_5$ PAMs comparable in potency to the parent, the known CYP_{450}-mediated in vivo ago-PAM metabolite, namely, VU0453103, was not formed. Thus, this technology platform has potential to identify hot spots for oxidative metabolism and produce active metabolites of small-molecule ligands in a high-throughput, scalable manner.

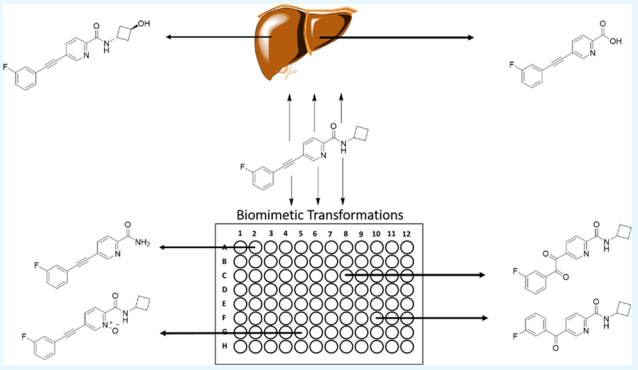

INTRODUCTION

From steep structure−activity relationships to family subtype selectivity issues to a potential lack of conservation of allosteric sites (e.g., functional activity) across species, allosteric GPCR drug discovery is fraught with challenges and development caveats.[1−4] However, no challenge is more daunting than that of "molecular switches", subtle structural changes to an allosteric ligand, often single-atom (e.g, introduction of a methyl, fluoro, amino, or hydroxyl moiety), that can reverse the mode of pharmacology (e.g., from a positive to a negative allosteric modulator, PAM to NAM, or vice versa) or change family subtype selectivity.[1−11] Fortunately, molecular switches are not present across all allosteric ligands but occur rather randomly within certain highly planar chemotypes, suggesting shallow induced fit pockets. While molecular switches have oftentimes been proven beneficial to gain entry to activity at a given receptor subtype (e.g., conversion of an $mGlu_4$ PAM to a selective $mGlu_1$ PAM[12] or an $mGlu_5$ PAM to a selective $mGlu_3$ NAM[13]), they can also convert a nontoxic "pure" $mGlu_5$ PAM (VU0403602, **1**) to neurotoxic $mGlu_5$ ago-PAM (VU0453103, **2**) in vivo via an unexpected CYP_{450}-mediated oxidation (Figure 1).[14] The latter is challenging to de-risk, without multiple in vivo studies, performed with and without CYP_{450} inhibitors, to ascertain parent and metabolite drug levels as well as neurotoxicity in rodent seizure models, and ultimately preparative CYP_{450} incubations to identify the structure of the neurotoxic metabolite.[14] Within a fast-moving lead optimization effort, employing an in vivo de-risking strategy is not practical in terms of time, cost, and the likelihood of success. Based on these realities, we were intrigued by newly available biomimetic oxidation (BMO) kits, advertised as a "synthetic liver", mimicking the oxidative metabolism of multiple CYP_{450} enzymes (e.g., synthetic metalloporphyrins).[15] Importantly, 96 individual synthetic livers are in each well of a 96 well plate,

Received: July 2, 2019
Accepted: July 17, 2019
Published: July 26, 2019

DOI: 10.1021/acsomega.9b02017
ACS Omega 2019, 4, 12782−12789

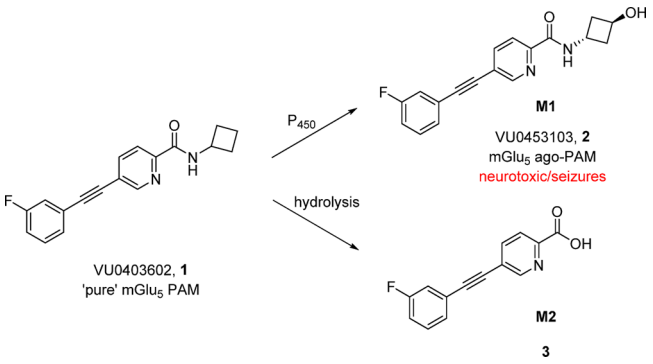

Figure 1. Major biotransformation of pure $mGlu_5$ PAM, namely, VU0403602 (**1**), to M1, a potent, neurotoxic $mGlu_5$ ago-PAM (VU0453103, **2**), and M2, the inactive product of amide hydrolysis **3** observed in male rat hepatic S9 fractions. Other minor metabolites were the corresponding *N*-oxide or result of oxidation of the acetylene moiety.

allowing an expansive survey of synthetic biotransformation of a ligand, coupled with production kits to readily scale the chemistry from any distinct well (e.g., synthetic CYP_{450}), enabling isolation and characterization of the "metabolite(s)".[12] If successful and productive, this could revolutionize our current, laborious approach to identifying allosteric ligand chemotypes susceptible to in vivo molecular switches and more readily focus optimization efforts on chemical series devoid of molecular switches.

RESULTS AND DISCUSSION

Knowing the in vitro and in vivo metabolism of **1**,[11] as well as the relevant CYP_{450}-mediated oxidative metabolites, we elected to assess the ability of a commercial BMO kit[15] to metabolize $mGlu_5$ PAM **1** and determine if any of the 96 synthetic livers could generate **2** or other known metabolites. Incubation of **1** with the screening BMO kit led to the production of only four metabolite-like compounds M3−M6 (Figure 2).[16] The

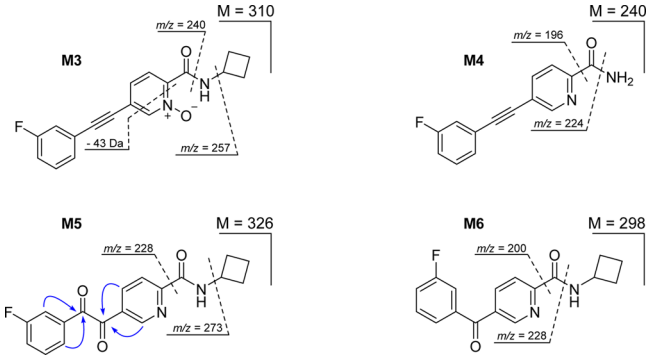

Figure 2. Observed key fragments of M3−M6. Key HMBC correlations in blue.

metabolite of greatest interest, the $mGlu_5$ ago-PAM **2**, produces a parent ion adduct of $[M + H]^+$ with *m*/*z* 311 and MS/MS produced the minor fragment of *m*/*z* 293 resulting from the loss of water (−18 Da; $-H_2O$), while the water loss fragment from **1** (*m*/*z* 295 $[M + H]^+$) results in a *m*/*z* of 277. The next major fragments of **2** result from, first, the loss of the cyclobutanol moiety producing an $[M - 71 + 2H]^+$ ion at *m*/*z* 241 and, second, fragmentation of the carbon nitrogen bond producing the benzoyl ion at *m*/*z* 223. For **1**, the fragments associated with the water-assisted hydrolysis of the amide bond and the loss of the cyclobutyl group are also observed in the MS/MS and MS/MS/MS (MS^3) at *m*/*z* 242 and *m*/*z* 241, respectively. The last major fragment observed in both **1** and **2** is the decarboxylation producing a fragment with a *m*/*z* of 196. Since a standard of **2** was available, we were able to determine via retention time analysis that no detectable amount of **2**, representing hydroxylation of the 3-position on the cyclobutyl moiety of **1**, was produced by any of the 96 individual synthetic metalloporphyrins in the BMO kit.[16]

The BMO screening kit did produce four other oxidative species, and analysis of the unknowns produced from **1** (M3−M6) were first analyzed by UPLC MS/MS/MS ($UPLCMS^3$).[16] The parent ion of M3 was observed as the $[M + H]^+$ adduct at *m*/*z* 311, and the first notable fragment from the MS/MS was the loss of water corresponding to the *m*/*z* at 293. The major fragment at *m*/*z* 257 resulted from the loss of the cyclobutyl moiety, which is an increase of 16 Da from the removal of the cyclobutyl moiety observed at *m*/*z* 241 in **1** and **2**. The next series of fragments at *m*/*z* 242 and 241 were the same fragments observed in **1** and **2**; however, a new fragment at *m*/*z* 240 represented the benzoyl ion fragment. This fragment at *m*/*z* 240 is also observed as the major fragment in the MS^3 of *m*/*z* 257. The remaining two fragments are decarboxylation and oxygen loss fragmentation at *m*/*z* 196 and an interesting fragment at *m*/*z* 214. This *m*/*z* 214 fragment corresponded to the loss of −43 Da from *m*/*z* 257, which would correspond to the loss of oxygen and hydrogen cyanide.[1] These fragments at *m*/*z* 257 and 240 indicate that the oxygen was not attached to the cyclobutyl moiety like in **2**, and thus, the fragment at *m*/*z* 214 indicates that there was a high likelihood that M3 is the *N*-oxide of **1**, a metabolite detected in small amounts from traditional metabolite identification (MetID) studies. A simple comparison of the retention time, fragmentation patterns, and coinjection (average of the coinjection retention time analysis t_R = 0.923 ± 0.000 min) with an available standard, synthesized to support the previous MetID studies, confirmed the identity of M3 as **4** (VU0409496), the *N*-oxide of **1** (Figure 3).[16]

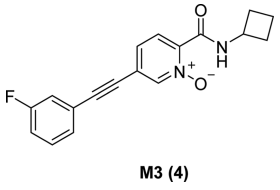

Figure 3. Confirmed structure of M3 as the *N*-oxide **4** (VU0409496).

The biomimetic kit afforded 3.3 mg of M4. $UPLCMS^3$ of M4 found a parent ion of $[M + H]^+$ at *m*/*z* 241, which corresponded to the primary amide of **1**. MS/MS of the parent ion gave two fragments, the water-assisted hydrolysis at *m*/*z* 242 and the major fragment at *m*/*z* 224, the benzoyl ion. The MS^3 of *m*/*z* 224 gave the decarboxylation fragment at *m*/*z* 196. All listed fragments indicate the identity of M4 as the primary amide of **1**. The ^1H NMR of M4 displayed the same seven aromatic proton signals observed in **1** and lacked signals corresponding to the cyclobutyl moiety.[16] The only extra signal observed is the result of an increased barrier of rotation due to the intramolecular hydrogen bond observed in picolinamides

DOI: 10.1021/acsomega.9b02017
ACS Omega 2019, 4, 12782−12789

Scheme 1. Synthesis of Putative Synthetic Metabolites M4−M6[a]

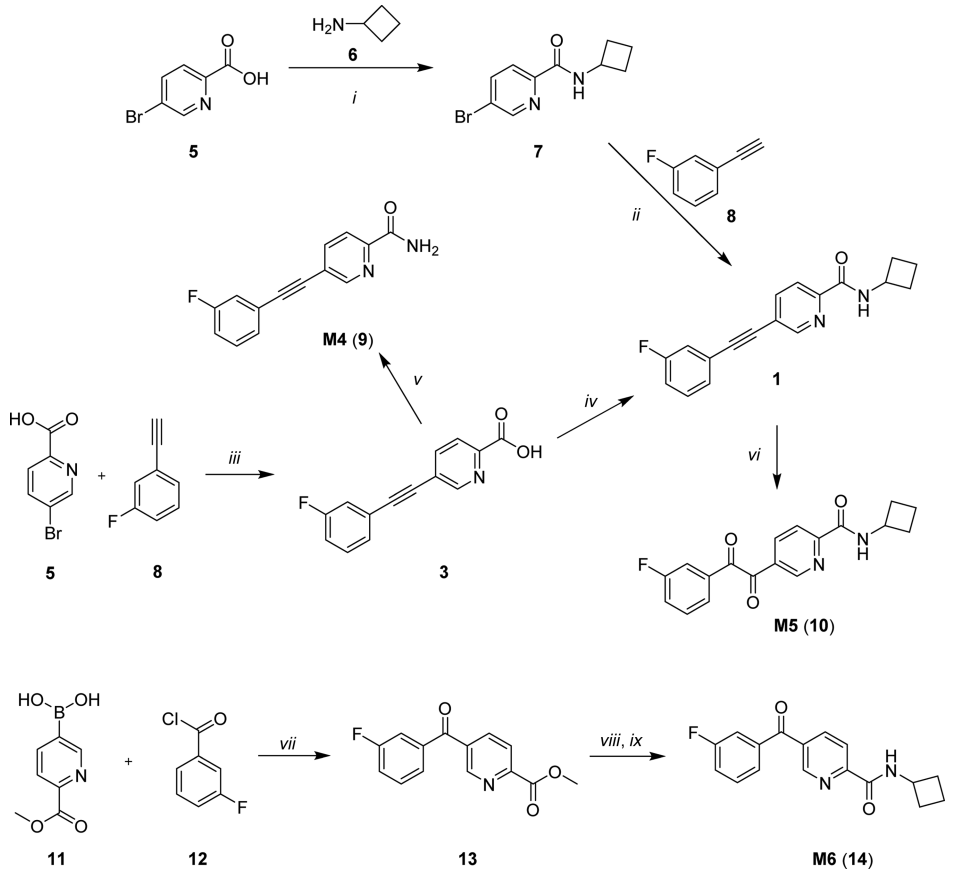

[a](i) HATU, DIPEA, DMF, rt, 30 min; 85%. (ii) CuI, DEA, DMF, 60 °C, 2 h, microwave; 80%. (iii) $Pd(PPh_3)_4$, CuI, DIPEA, DMF, 60 °C, microwave, 45 min; 56%. (iv) **6**, HATU, DIPEA, DMF, rt, 1 h; 76%. (v) EDAC, DIPEA, hydroxybenzotriazole, $(NH_4)_2CO_3$, THF, rt, 2 h; 32%. (vi) $MgSO_4$, $KMnO_4$, $NaHCO_3$, acetone/H_2O, rt, 1 h; 21%. (vii) $Pd(PPh_3)_4$, K_2CO_3, THF/H_2O, 65 °C, 16 h; 8%. (viii) NaOH, DMF/H_2O, 60 °C, 2 h. (ix) **6**, HATU, DIPEA, DMF, rt, 1 h; 16% over two steps.

resulting in the primary amide having two unique signals at δ_H 7.80 (1H, br s, NH) and δ_H 5.69 (1H, br s, NH).[17]

The biomimetic kit also afforded 1.8 mg of M5. UPLCMS^3 of M5 found a parent ion of $[M + H]^+$ at m/z 327, which corresponds to the addition of two oxygens to **1** (+32 Da; +O × 2). The first fragment resulted from the loss of water with m/z 309. The familiar loss of the cyclobutyl moiety and the water-assisted hydrolysis fragments were present at m/z 273 and 274; however, both fragments were still +32 Da heavier than **1** (m/z 241 and 242) when these same losses occurred. MS^3 of the major fragment m/z 273 indicated the loss of ammonia (−17 DA; $-NH_3$) to afford the benzoyl ion at m/z 256 followed by the loss of hydrogen cyanide (−27 Da; −HCN) at m/z 246 and decarboxylation at m/z 228, all of which are still +32 Da heavier than their counterpart's fragments from **1**. These observations indicated that the two oxygens must be attached to the phenylethynylpyridine moiety and not as the *N*-oxide since HCN was lost and both oxygens still remained.[16]

The ^{1}H NMR spectrum of M5 was obtained to hopefully glean more structural information. The chemical shifts as expected for the cyclobutyl moiety remain constant. The proton resonances from the picolinamide and the 2-fluorobenzyl moiety were all deshielded up to δ_H 9.11 (1H, br dd, J = 2.1, 0.8 Hz), 8.42 (1H, dd, J = 8.1, 2.1 Hz), 8.34 (1H, dd, J = 8.2, 0.8 Hz), 7.78 (1H, dt, J = 7.8, 1.3 Hz), 7.74 (1H, ddd, J = 8.8, 2.7, 1.6 Hz), 7.53 (1H, td, J = 8.4, 5.2 Hz), and 7.41 (1H, td, J = 16.6, 2.6 0.9 Hz) in M3 from δ_H 8.66 (1H, br s), 8.18 (1H, d, J = 8.0 Hz), 7.94 (1H, dd, J = 8.0, 2.0 Hz), 7.39−7.31 (2H, m), 7.25 (1H, dd, J = 9.7, 2.8 Hz), and 7.15−7.06 (1H, m) observed in **1**. The only exchangeable signal observed was the amide NH proton at δ_H 8.17 (1H, br d, J = 7.9 Hz). The ^{1}H NMR revealed that no carbon−hydrogen bonds were replaced with carbon−oxygen bonds, indicating the ethynyl moiety as the most likely position for the addition of the two oxygens. In order to determine if oxidation occurred at the triple bond, an HMBC spectrum of M5 was obtained. Careful examination of the HMBC correlations from two of the picolinamide protons at δ_H 9.11 and δ_H 8.42 shows that they both display correlations to a ketone at δ_C 191.1, while two protons from the 2-fluorobenzyl moiety at δ_H 7.78 and δ_H 7.74 both display correlations to a ketone at δ_C 191.0. These observations support the transformation of the triple bond into a di-ketone assigning the potential structure as M5.[16]

The biomimetic kit provided only 0.5 mg of M6, which was found to have a parent ion of $[M + H]^+$ m/z 299. This mass was rather interesting since it was only 4 Da higher in mass than **1**, which indicated that functionalities were lost and added. Notable fragments observed in the MS/MS were the loss of water at m/z 288 (−18 Da; $-H_2O$) and the loss of the cyclobutyl moiety $[M - 55 + 2H]^+$ to afford the major fragment at m/z 245. Further fragmentation (MS^3) of m/z 245

DOI: 10.1021/acsomega.9b02017
ACS Omega 2019, 4, 12782−12789

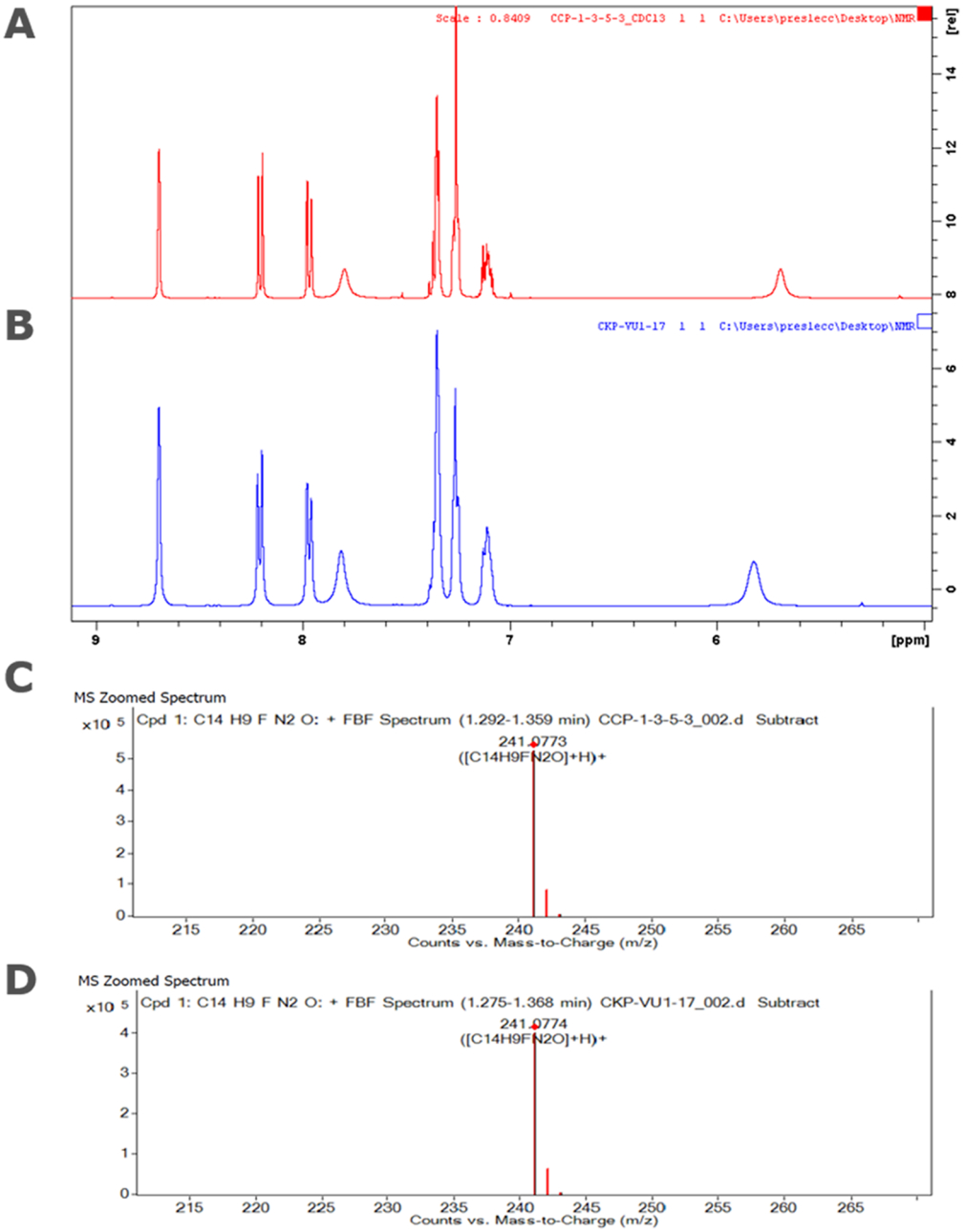

Figure 4. Comparison of data from isolated M4 (**9**) from the BMO kit and synthetic **9**. (A) ^{1}H NMR (400 MHz) of M4 (**9**) from the BMO kit stacked on top of (B) ^{1}H NMR (400 MHz) of M4 (**9**) prepared via synthesis. (C) HRMS ESI of M4 (**9**) from the BMO kit and (D) the HRMS ESI of synthetic **9**.

resulted in the formation of the water-assisted amide hydrolysis product at m/z 246, the loss of ammonia to form the benzoyl ion (−17 Da; $-NH_3$) at m/z 228, loss of hydrogen cyanide (−27 Da; −HCN) at m/z 218, and decarboxylation at m/z 200. Assuming that a carbon was lost and adding 12 Da to m/z 299 gives a m/z of 311 indicate that there is a high likelihood that a carbon was removed. Since all lost fragments have been identified as fragments lost from M3−M5 and since the added oxygen was still present after decarboxylation, the lost carbon and the added oxygen must be distinct from the phenylethynylpyridine moiety. Examination of the ^{1}H NMR shows that the cyclobutyl moiety and amide proton remain unchanged and all seven protons from the picolinamide and 2-fluorobenzyl were still present at δ_H 8.92 (1H, br d, J = 1.6 Hz), 8.33 (1H, d, J = 8.1 Hz), 8.22 (1H, dd, J = 8.1, 2.1 Hz), 7.60−7.47 (3H, m), and 7.36 (1H, tdd, J = 8.1, 2.6, 1.3 Hz).[13] Since the cyclobutyl moiety, picolinamide, and the 2-fluorobenzyl moiety were not modified, it left the ethynyl linkage as the only possible place for modification. If the ethynyl linkage was replaced with a ketone, then the loss of a carbon and the addition of an oxygen would be accounted for. It has also been shown to be possible to convert internal alkynes into shorter ketones with the use of porphyrins.[18] This assumption would assign the structure as M6.[16]

In order to unambiguously confirm the structures and identities of M4−M6, we synthesized de novo these putative synthetic metabolites and compared spectral data and retention times (Scheme 1). Starting from commercial acid

DOI: 10.1021/acsomega.9b02017
ACS Omega 2019, 4, 12782−12789

5, a HATU-mediated amide coupling with cyclobutyl amine **6** afforded amide **7** in 85% yield.[19] A Sonogashira coupling between **7** and 3-fluorophenyl acetylene **8** provided **1** in 56% yield. Alternatively, **1** was also prepared via a different route. Direct Sonogashira coupling of acid **5** with **8** delivered acid **3**, which could then be employed to access **1** via a standard amide coupling. Acid **3** can also be employed to give the primary carboxamide M4 (**9**) via an amide coupling sequence with $(NH_4)_2CO_3$, albeit in only 32% yield.[20] Following a known literature protocol,[21] the acetylene moiety in **1** was smoothly converted to the diketone M5 (**10**) by treatment with $KMnO_4$. The last putative metabolite M6 (**14**) was accessed in two steps. A palladium-catalyzed acylation between boronic acid **11** and acid chloride **12** gave ketone **13** in low yield. Hydrolysis of the acid and another HATU-mediated amide coupling with **6** delivered M6 (**14**) in low yield over two steps (16%).

To confirm the structure of M4 as the primary amide of **1**, it was synthesized (Scheme 1) and compared via retention time, fragmentation patterns, coinjection, and ^{1}H NMR comparison (see the Supporting Information).[16] The comparison analysis confirmed M4 as **9** (average of the coinjection retention time analysis t_R = 1.047 ± 0.001 min), the primary amide of **1** (Figure 4).[16] Similarly, the proposed structure of M5, diketone **10**, was synthesized on scale (Scheme 1) to aid in the confirmation of the structure. The analysis of the retention time (average of the coinjection retention time analysis t_R = 0.957 ± 0.001 min), fragmentation patterns, coinjection, and ^{1}H NMR comparison confirmed the identity of M5 as the diketone **10**.[16] Once again, to confirm the proposed structure of M6, **14** was synthesized on scale (Scheme 1). Analysis of the retention time (average of the coinjection retention time analysis t_R = 0.969 ± 0.001 min), mass fragmentation patterns, coinjection, and ^{1}H NMR confirmed **14** as the structure for M4.[16] With M3−M6 in hand, they were evaluated in our standard $mGlu_5$ calcium mobilization functional assay, and M5 and M6 were inactive in both PAM and NAM modes; however, M3 and M4 proved more interesting.

The *N*-oxide, M3 (**4**, VU0409496) proved to be a potent, pure PAM in our standard screening assays (human EC_{50} = 38.7 nM, pEC_{50} = 7.41 ± 0.06, 71.5 ± 2.6% Glu Max; rat EC_{50} = 28 nM, pEC_{50} = 7.55 ± 0.06, 58.5 ± 3.6% Glu Max), roughly equipotent to the parent **1** and similarly devoid of $mGlu_5$ agonism (human EC_{50} > 30 μM). This active metabolite was produced in very small quantities in native systems, but the BMO kit produced M3 in a significant amount to warrant characterization. Further evaluation of M3 found it to be non-CNS penetrant, with modest fraction unbound (f_u (*h*, *r*) = 0.012, 0.033) and a metabolic activator of 3A4; therefore, M3 was not viable as a lead. The primary carboxamide M4 (VU6025968), a new synthetic oxidative metabolite not observed in native systems, was also an active $mGlu_5$ PAM. As we have sufficient quantity from the BMO production kit, we screened both the kit-produced M4 and synthetic M4 in the human $mGlu_5$ assay. The kit-produced M4 afforded a pure PAM profile, with an EC_{50} of 510 nM (75% Glu Max), and the synthetic-derived M4 was equivalent (EC_{50} = 315 nM, 77%, and no agonism noted up to 30 μM). Importantly, it was significant to identify active oxidative metabolites from the BMO kit that retained the desired mode of pharmacology (pure PAM versus ago-PAM) that were either produced in minor quantities or not observed in classical native system preparations.

CONCLUSIONS

In summary, the BMO kit proved to afford a highly expedient synthetic liver producing a number of known metabolites of **1**, as well as novel synthetic metabolites in quantities sufficient for full characterization and biological assessment. MetID studies of the synthetic analogs were confirmed by independent synthesis, and unexpectedly based on the structures of M3−M6, two were potent pure $mGlu_5$ PAMs, that is, active metabolites. We hoped that the BMO kit would produce the potent, neurotoxic $mGlu_5$ ago-PAM (VU0453103, **2**) of pure PAM **1**, the result of an oxidative-metabolism-induced molecular switch; however, this was not observed in any of the 96 individual synthetic livers. Still, the technology platform has utility in producing on scale synthetic oxidative metabolites, but the biomimetic catalysts (e.g., metalloporphyrins) may not fully encompass all of the oxidative chemistry of endogenous CYP_{450}s. Further work in this arena is in progress, and additional studies with other allosteric ligands will be reported in due course.

EXPERIMENTAL SECTION

General Methods. All reactions were carried out employing standard chemical techniques under air unless noted. Solvents used for extraction, washing, and chromatography were HPLC-grade. All reagents were purchased from commercial sources and were used without further purification. All microwave reactions were carried out in sealed tubes in a Biotage Initiator microwave synthesis reactor. Analytical HPLC was performed on an Agilent 1200 LCMS with a gradient of 5−95% MeCN in 0.1% TFA water over 1.5 min and UV detection at 215 and 254 nm along with ELSD detection and electrospray ionization, with all final compounds showing >95% purity. High-resolution mass spectra were obtained on an Agilent 6540 UHD Q-TOF with the ESI source. Automated flash column chromatography was performed on a Teledyne ISCO Combi-Flash system. Reversed-phase HPLC was performed on a Gilson preparative reversed-phase HPLC system comprising a 333 aqueous pump with solvent-selection valve, 334 organic pump, GX-271 or GX-281 liquid handler, two column switching valves, and a 155 UV detector. The UV wavelength for fraction collection was user-defined, with absorbance at 254 nm always monitored. The column used was Phenomenex Axia-packed Gemini C_{18} (30 × 50 mm, 5 μm). For the acidic method, the mobile phase was CH_3CN in H_2O (0.1% TFA). Gradient conditions were 0.75 min equilibration followed by a user-defined gradient (starting organic percentage, ending organic percentage, duration), held at 95% CH_3CN in H_2O (0.1% TFA) for 1 min, 50 mL/min, 23 °C. For the basic method, the mobile phase was CH_3CN in H_2O (0.05% v/v NH_4OH). Gradient conditions were 0.75 min equilibration followed by a user-defined gradient (starting organic percentage, ending organic percentage, duration), held at 95% CH_3CN. $LCMS^3$ experiments were carried out on an Agilent 1290 UPLC system coupled to a Thermo Scientific LTQ XL Linear Ion trap mass spectrometer using CH_3CN and 10 mM ammonium formate with pH adjusted to 4.1 as the mobile phases with a Phenomenex Kinetex C_{18} (2.6 μ, 2.1 × 50 mm, 100 Å column) held at 50 °C with a CERA Temperature Controller at 1 mL/min. All NMR spectra were recorded on a 400 MHz Bruker AV-400 instrument. ^{1}H chemical shifts are reported as δ values in ppm relative to the residual solvent peak ($CDCl_3$ =

DOI: 10.1021/acsomega.9b02017
ACS Omega 2019, 4, 12782−12789

7.26, DMSO-d_6 = 2.50, CD_3OD = 4.78). Data are reported as follows: chemical shift, multiplicity (br = broad, s = singlet, d = doublet, t = triplet, q = quartet, dd = doublet of doublets, dt = doublet of triplets, ddd = doublet of doublet of doublets, ddq = doublets of doublets of quartets, sext = sextet, m = multiplet), coupling constant (Hz), and integration. ^{13}C chemical shifts are reported as δ values in ppm relative to the residual solvent peak ($CDCl_3$ = 77.2, DMSO-d_6 = 39.5, CD_3OD = 49.15).

Compound Information. *5-Bromo-N-cyclobutylpicolinamide (**7**).* To a vial were added 5-bromopicolinic acid (**5**) (1.24 mmol), HATU (1.49 mmol), DMF (5 mL), DIPEA (4.95 mmol), and cyclobutylamine (**6**) (1.49 mmol). The mixture was allowed to stir for 30 min at rt after which time LCMS indicated product formation. The sample was filtered and purified on normal-phase chromatography using 0−20% EtOAc in hexanes to give 5-bromo-*N*-cyclobutylpicolinamide (**7**) as a white solid (85% yield). ^1H NMR (400 MHz, $CDCl_3$) δ 8.58 (1H, dd, J = 2.2, 0.6 Hz), 8.06 (1H, dd, J = 8.3, 0.6 Hz), 8.01 (1H, br s), 7.95 (1H, dd, J = 8.3, 2.2 Hz), 4.62−4.51 (1H, m), 2.47−2.37 (2H, m), 2.09−1.97 (2H, m), 1.83−1.73 (2H, m); ^{13}C NMR (100 MHz, $CDCl_3$) δ 162.6, 149.3, 148.6, 140.1, 124.0, 123.8, 44.8, 31.3, 15.4; LCMS: t_R = 0.855 min (>98%); m/z = 256.3 $[M + H]^+$; HRMS (ESI) m/z $[M + H]^+$ calcd for $C_{10}H_{12}BrN_2O^+$ 255.0128, found 255.0126.

*5-((3-Fluorophenyl)ethynyl)picolinic Acid (**3**).* In a microwave vial were added 5-bromopicolinic acid (**5**) (4.95 mmol), tetrakis(triphenylphosphine)palladium(0) (0.250 mmol), 3-fluorophenylacetylene (**8**) (5.94 mmol), copper(I) iodide (0.50 mmol), diethylamine (29.7 mmol), and DMF (7 mL). The mixture was heated in the microwave at 60 °C for 45 min. The mixture was basified with saturated aqueous $NaHCO_3$ and diluted with 5 mL of DCM. The aqueous layer was collected and acidified with 2 N HCl (pH 1−2). The acidified mixture was extracted with $CHCl_3$, dried over anhydrous sodium sulfate, and concentrated via vacuum. The resulting residue was purified on normal-phase chromatography using 0−10% DCM in MeOH to give 5-((3-fluorophenyl)ethynyl)picolinic acid (**3**) as a yellow solid (56% yield). ^1H NMR (400 MHz, DMSO-d_6) δ 13.42 (1H, br s), 8.88 (1H, dd, J = 2.1, 0.7 Hz), 8.15 (1H, dd, J = 8.1, 2.1 Hz), 8.08 (1H, dd, J = 8.1, 0.7 Hz), 7.53−7.46 (3H, m), 7.37−7.32 (1H, m). ^{13}C NMR (100 MHz, DMSO-d_6) δ 165.6, 161.8 (d, $^1J_{C-F}$ = 243.5 Hz), 151.5, 147.4, 139.8, 131.1 (d, $^3J_{C-F}$ = 8.8 Hz), 128.0 (d, $^4J_{C-F}$ = 2.8 Hz), 124.4, 123.2 (d, $^3J_{C-F}$ = 9.7 Hz), 122.0, 118.3 (d, $^2J_{C-F}$ = 23.1 Hz), 117.0 (d, $^2J_{C-F}$ = 21 Hz), 93.2 (d, $^4J_{C-F}$ = 3.4 Hz), 86.5. LCMS: t_R = 0.794 min (>98%) m/z = 242.2 $[M + H]^+$; HRMS (ESI) m/z $[M + H]^+$ calcd for $C_{14}H_9FNO_2^+$ 242.0612, found 242.0613.

*N-Cyclobutyl-5-((3-fluorophenyl)ethynyl)picolinamide (**1**).* Route 1: To a microwave vial were added 5-bromo-*N*-cyclobutylpicolinamide (**7**) (0.98 mmol), *trans*-dichlorobis-(tripheylphosphine)palladium (II) (0.20 mmol), copper (I) iodide (0.20 mmol), DMF (4 mL), and DIPEA (9.80 mmol). The vial was capped and purged with N_2, and then 3-fluorophenylacetylene (**8**) (4.90 mmol) was added. The vial was heated to 60 °C in a microwave for 2 h after which time LCMS indicated product formation. The sample was filtered, concentrated, and resuspended in DMSO. The sample was purified on reversed-phase chromatography using 60−95% ACN in H_2O/0.05% NH_4OH to give *N*-cyclobutyl-5-((3-fluorophenyl)ethynyl)picolinamide (**1**) as an off-white solid (80% yield).

Route 2: 5-((3-Fluorophenyl)ethynyl)picolinic acid (**3**) (0.331 mmol) was dissolved in DMF (0.580 mL). DIPEA (0.660 mmol) was added, and the reaction solution was stirred for 30 min. HATU (0.400 mmol) was added, and the reaction solution was stirred for 30 min. Cyclobutylamine (**6**) (0.400 mmol) was added, and the reaction solution was stirred for 1 h at rt. At completion, the reaction solution was filtered and purified by reversed-phase chromatography to give *N*-cyclobutyl-5-((3-fluorophenyl)ethynyl)picolinamide (**1**) as an off-white solid (76% yield). ^1H NMR (400 MHz, $CDCl_3$) δ 8.68 (1H, s), 8.18 (1H, d, J = 8.1 Hz), 8.10 (1H, br d, J = 7.5 Hz), 7.94 (1H, dd, J = 2.0, 8.1 Hz), 7.39−7.31 (2H, m), 7.28−7.22 (1H, m), 7.16−7.09 (1H, m), 4.62 (1H, sext, J = 8.2 Hz), 2.51−2.41 (2H, m), 2.15−2.02 (2H, m), 1.88−1.76 (2H, m); ^{13}C NMR (100 MHz, $CDCl_3$) δ 162.7, 162.6 (d, $^1J_{C-F}$ = 247.5 Hz), 150.5, 148.8, 140.0, 130.3 (d, $^3J_{C-F}$ = 8.6 Hz), 127.8 (d, $^4J_{C-F}$ = 3.0 Hz), 124.1 (d, $^3J_{C-F}$ = 9.6 Hz), 122.6, 121.8, 118.7 (d, $^2J_{C-F}$ = 23.0 Hz), 116.7 (d, $^2J_{C-F}$ = 21.1 Hz), 93.4 (d, $^4J_{C-F}$ = 3.6 Hz), 86.5, 44.8, 31.3 (double intensity), 15.4; $[M + H]^+$; HRMS (ESI) m/z $[M + H]^+$ calcd for $C_{18}H_{16}FN_2O^+$ 295.1241, found 295.1248.

*5-((3-Fluorophenyl)ethynyl)-N-((1R,3R)-3-hydroxycyclobutyl)picolinamide (**2**).* The compound was available as a 10 mM DMSO stock solution from previous work conducted by VCNDD. Synthesis and chiral resolution were previously reported.[11]

*N-Cyclobutyl-5-((3-fluorophenyl)ethynyl)picolinamide N-Oxide (M3, **4**).* The compound was available as a 10 mM DMSO stock solution from previously patented work at VCNDD.[18]

*5-((3-Fluorophenyl)ethynyl)picolinamide (M4, **9**).* 5-((3-Fluorophenyl)ethynyl)picolinic acid (**3**) (0.210 mmol), 1-(3-dimethylaminopropyl)-3-ethylcarbodiimide hydrochloride (0.230 mmol), and 1-hydroxybenzotriazole (0.230 mmol) were dissolved in THF (1.8 mL). DIPEA (0.230 mmol) was added, and the reaction solution was stirred for 10 min at rt. Ammonium carbonate (0.620 mmol) was added, and the reaction solution was stirred overnight at rt. Solvent was concentrated via vacuum, a 1:1 saturated aqueous sodium bicarbonate/water solution (1.5 mL) was added, and the reaction solution was stirred for 2 h. The product was filtered, and the solvent was concentrated via vacuum. The resulting residue was purified by reversed-phase chromatography to give 5-((3-fluorophenyl)ethynyl)picolinamide (M4, **9**) as a white solid (32% yield). ^1H NMR (400 MHz, $CDCl_3$) δ 8.70 (1H, br d, J = 2.0 Hz), 8.21 (1H, dd, J = 0.6, 8.1 Hz), 7.97 (1H, dd, J = 2.0, 8.1 Hz), 7.81 (1H, br s), 740−7.32 (2H, m), 7.29−7.23 (1H, m), 7.16−7.06 (1H, m), 5.70 (1H, brs); ^{13}C NMR (100 MHz, $CDCl_3$) δ 166.1, 162.5 (d, $^1J_{C-F}$ = 247.5 Hz), 150.8, 148.2, 140.0, 130.5 (d, $^3J_{C-F}$ = 8.7 Hz), 127.9 (d, $^4J_{C-F}$ = 3.2 Hz), 124.0 (d, $^3J_{C-F}$ = 9.4 Hz), 123.1, 122.1, 118.7 (d, $^2J_{C-F}$ = 23.2 Hz), 116.8 (d, $^2J_{C-F}$ = 21.2 Hz), 93.7 (d, $^4J_{C-F}$ = 3.5 Hz), 86.4; LCMS: t_R = 0.824 min (98%) m/z = 241.0 $[M + H]^+$; HRMS (ESI) m/z $[M + H]^+$ calcd for $C_{14}H_{10}FN_2O^+$ 241.0772, found 241.0774.

*N-Cyclobutyl-5-(2-(3-fluorophenyl)-2-oxoacetyl)-picolinamide (M5, **10**).* *N*-Cyclobutyl-5-((3-fluorophenyl)-ethynyl)picolinamide (**1**) (0.025 mmol) was dissolved in acetone (2 mL). A suspension of sodium bicarbonate (0.130 mmol) and magnesium sulfate (43 mg, 0.350 mmol) in water (0.74 mL) was added followed by potassium permanganate (87 mg, 0.550 mmol). The reaction solution was stirred for 1 h at rt. At completion, hexanes were added (5 mL), and the

DOI: 10.1021/acsomega.9b02017
ACS Omega 2019, 4, 12782−12789

solution was decanted. The remaining residue was purified by reversed-phase chromatography to give *N*-cyclobutyl-5-(2-(3-fluorophenyl)-2-oxoacetyl)picolinamide (M5, **10**) as a yellow solid (21% yield). ^{1}H NMR (400 MHz, $CDCl_3$) δ 9.11 (1H, dd, J = 0.8, 2.1 Hz), 8.42 (1H, dd, J = 2.1, 8.2 Hz), 8.33 (1H, dd, J = 0.8, 8.2 Hz), 8.17 (1H, br d, J = 7.9 Hz), 7.78 (1H, dt, J = 1.4, 7.8 Hz), 7.74 (1H, ddd, J = 1.6, 2.7, 8.8 Hz), 4.60 (1H, sext, J = 8.1 Hz), 2.49−2.39 (2H, m), 2.12−1.99 (2H, m), 1.86−1.74 (2H, m); ^{13}C NMR (100 MHz, $CDCl_3$) δ 191.1, 191.0 (d, $^4J_{C-F}$ = 2.3 Hz), 163.0 (d, $^1J_{C-F}$ = 250.0 Hz), 161.9, 154.1, 149.8, 138.9, 134.4 (d, $^3J_{C-F}$ = 6.6 Hz), 131.1 (d, $^4J_{C-F}$ = 7.7 Hz), 130.1, 126.4 (d, $^4J_{C-F}$ = 3.1 Hz), 122.7 (d, $^2J_{C-F}$ = 21.4 Hz), 122.5, 116.6 (d, $^2J_{C-F}$ = 22.8 Hz), 44.9, 31.2 (double intensity), 15.4; LCMS: t_R = 1.028 min (>98%), m/z = 327.4 $[M + H]^+$; HRMS (ESI) m/z $[M + H]^+$ calcd for $C_{18}H_{16}FN_2O_3^+$ 327.1139, found 327.1143.

*Methyl 5-(3-Fluorobenzoyl)picolinate (**13**).* Methyl picolinate-5-boronic acid (**11**) (0.570 mmol), 3-fluorobenzoyl chloride (**12**) (0.470 mmol), potassium carbonate (1.420 mmol), and tetrakis(triphenylphosphine)palladium(0) (0.0500 mmol) were placed in a vial that was purged with N_2. THF (2.1 mL) and water (0.30 mL) were added, and the reaction solution was heated overnight at 65 °C. The reaction solution was filtered through Celite and washed with EtOAc, and the solvent was concentrated via vacuum. The resulting residue was purified on normal-phase chromatography using 0−80% EtOAc in hexanes to give methyl 5-(3-fluorobenzoyl)picolinate (**13**) as a white solid (8% yield). ^{1}H NMR (400 MHz, CD_3OD) δ 8.91 (1H, dd, J = 2.1, 0.8 Hz), 8.26 (1H, dd, J = 8.1, 2.1 Hz), 8.21 (1H, dd, J = 8.1, 0.8 Hz) 7.53 (3H, m), 7.39 (1H, m), 3.94 (3H, s); ^{13}C NMR (100 MHz, CD_3OD) δ 194.1 (d, $^4J_{C-F}$ = 2.2 Hz), 165.9, 164.2 (d, $^1J_{C-F}$ = 247.4 Hz), 151.3, 140.3, 139.9 (d, $^3J_{C-F}$ = 6.6 Hz), 137.2, 132.1 (d, $^3J_{C-F}$ = 7.8 Hz), 127.4 (d, $^4J_{C-F}$ = 3.0 Hz), 126.1, 121.7 (d, $^2J_{C-F}$ 21.6 Hz), 117.5 (d, $^2J_{C-F}$ = 22.8 Hz), 53.7; LCMS: t_R = 0.658 min (>98%), m/z = 260.2 $[M + H]^+$.

*N-Cyclobutyl-5-(3-fluorobenzoyl)picolinamide (M6, **14**).* Methyl 5-(3-fluorobenzoyl)picolinate (**13**) (0.041 mmol) was dissolved in a 1:1 solution of DMF/water (0.5 mL). Sodium hydroxide (0.122 mmol) was added, and the reaction solution was stirred at 60 °C for 30 min. At completion, as determined by LCMS, the reaction solution was acidified with 2 N HCl (pH = 4−5) and extracted with DCM. Organic fractions were dried over anhydrous sodium sulfate and concentrated via vacuum. The resulting crude carboxylic acid was used immediately in the next step, being dissolved in 0.1 mL of DMF, followed by the addition of DIPEA (0.082 mmol) and stirring for 30 min. HATU (0.049 mmol) was added, and the reaction solution was stirred for 30 min. Cyclobutylamine (0.049 mmol) was then added, and the reaction solution was stirred for 1 h at rt. At completion, the reaction solution was filtered and purified by reversed-phase chromatography to give *N*-cyclobutyl-5-(3-fluorobenzoyl)picolinamide (M6, **14**) as a clear oil (16% yield in two steps). ^{1}H NMR (400 MHz, $CDCl_3$) δ 8.92 (1H, dd, J = 0.6, 2.0 Hz), 8.32 (1H, dd, J = 0.6, 8.1 Hz), 8.21 (1H, dd, J = 2.1, 8.1 Hz), 8.21−8.15 (1H, m), 7.61−7.48 (3H, m), 7.40−7.32 (1H, m), 4.62 (1H, sext, J = 8.4 Hz), 2.51−2.40 (2H, m), 2.13−2.01 (2H, m), 1.86−1.75 (2H, m); ^{13}C NMR (100 MHz, $CDCl_3$) δ 193.1 (d, $^4J_{C-F}$ = 2.0 Hz), 162.9 (d, $^1J_{C-F}$ = 249.5 Hz), 162.3, 152.6, 149.2, 138.8, 138.6 (d, $^3J_{C-F}$ = 6.5 Hz), 134.6, 130.6 (d, $^3J_{C-F}$ = 7.8 Hz), 126.0 (d, $^4J_{C-F}$ = 3.0 Hz), 122.1, 120.7 (d, $^2J_{C-F}$ = 21.3 Hz), 116.8 (d, $^2J_{C-F}$ = 22.7 Hz), 44.9, 31.3 (double intensity), 15.4; LCMS: t_R = 0.899 min (>98%), m/z = 299.2 $[M + H]^+$; HRMS (ESI) m/z $[M + H]^+$ calcd for $C_{17}H_{16}FN_2O_2^+$ 299.1190, found 299.1196.

■ ASSOCIATED CONTENT

Supporting Information

The Supporting Information is available free of charge on the ACS Publications website at DOI: 10.1021/acsomega.9b02017.

Comparison of LCMS data for BMO kit-derived compounds M4−M6 and synthetic standards **4**, **9**, **10**, and **14** and copies of ^{1}H and ^{13}C NMR spectra for all synthetic compounds (PDF)

■ AUTHOR INFORMATION

Corresponding Author

*E-mail: craig.lindsley@vanderbilt.edu. Phone: 615-322-8700.

ORCID

Charles K. Perry: 0000-0001-9835-3434

Craig W. Lindsley: 0000-0003-0168-1445

Notes

The authors declare no competing financial interest.

■ ACKNOWLEDGMENTS

We thank William K. Warren, Jr., and the William K. Warren Foundation, who funded the William K. Warren Jr. Chair in Medicine (to C.W.L.).

■ REFERENCES

(1) Lindsley, C. W.; Emmitte, K. A.; Hopkins, C. R.; Bridges, T. M.; Gregory, K. A.; Niswender, C. M.; Conn, P. J. Practical strategies and concepts in GPCR allosteric modulator discovery: Recent advances with metabotropic glutamate receptors. *Chem. Rev.* **2016**, *116*, 6707−6741.

(2) Lindsley, C. W. 2013 Philip S. Portoghese Medicinal Chemistry Lectureship: Drug Discovery Targeting Allosteric Sites. *J. Med. Chem.* **2014**, *57*, 7485−7498.

(3) Wenthur, C. J.; Gentry, P. R.; Mathews, T. P.; Lindsley, C. W. Drugs for allosteric sites on receptors. *Annu. Rev. Pharmacol. Toxicol.* **2014**, *54*, 165−184.

(4) Conn, P. J.; Lindsley, C. W.; Meiler, J.; Niswender, C. M. Opportunities and challenges in the discovery of allosteric modulators of GPCRs for treating CNS disorders. *Nat. Rev. Drug Discovery* **2014**, *13*, 692−708.

(5) Engers, D. W.; Lindsley, C. W. Allosteric modulation of Class C GPCRs: A novel approach for the treatment of CNS disorders. *Drug Discovery Today: Technol.* **2013**, *10*, e269−e276.

(6) Wood, M. R.; Hopkins, C. R.; Brogan, J. T.; Conn, P. J.; Lindsley, C. W. "Molecular switches" on mGluR allosteric ligands that modulate modes of pharmacology. *Biochemistry* **2011**, *50*, 2403−2410.

(7) Sharma, S.; Kedrowski, J.; Rook, J. M.; Smith, R. L.; Jones, C. K.; Rodriguez, A. L.; Conn, P. J.; Lindsley, C. W. Discovery of Molecular Switches that Modulate Modes of Metabotropic Glutamate Receptor Subtype 5 (mGlu5) Pharmacology *In Vitro* and *In Vivo* Within a Series of Functionalized, Regioisomeric 2- and 5-(phenylethynyl)-pyrimidines. *J. Med. Chem.* **2009**, *52*, 4103−4106.

(8) Rodriguez, A. L.; Grier, M. D.; Jones, C. K.; Herman, E. J.; Kane, A. S.; Smith, R. L.; Williams, R.; Zhou, Y.; Marlo, J. E.; Days, E. L.; Blatt, T. N.; Jadhav, S.; Menon, U. N.; Vinson, P. N.; Rook, J. M.; Stauffer, S. R.; Niswender, C. M.; Lindsley, C. W.; Weaver, C. D.; Conn, P. J. Discovery of novel allosteric modulators of metabotropic glutamate receptor subtype 5 reveals chemical and functional diversity and in vivo activity in rat behavioral models of anxiolytic and antipsychotic activity. *Mol. Pharmaceutics* **2010**, *78*, 1105−1123.

DOI: 10.1021/acsomega.9b02017
ACS Omega 2019, 4, 12782−12789

(9) Schann, S.; Mayer, S.; Franchet, C.; Frauli, M.; Steinberg, E.; Thomas, M.; Baron, L.; Neuville, P. Chemical switch of a metabotropic glutamate receptor 2 silent allosteric modulator into dual metabotropic glutamate receptor 2/3 negative/positive allosteric modulators. *J. Med.Chem.* **2010**, *53*, 8775−8779.
(10) Mohr, K.; Schmitz, J.; Schrage, R.; Trankle, C.; Holzgrabe, U. Molecular Alliance—From Orthosteric and Allosteric Ligands to Dualsteric/Bitopic Agonists at G Protein Coupled Receptors. *Angew. Chem., Int. Ed.* **2013**, *52*, 508−516.
(11) Trzaskowski, B.; Latek, D.; Yuan, S.; Ghoshdastider, U.; Debinski, A.; Filipek, S. Action of Molecular Switches in GPCRs - Theoretical and Experimental Studies. *Curr. Med. Chem.* **2012**, *19*, 1090−1109.
(12) Cho, H. P.; Garcia-Barrantes, P. M.; Brogan, J. T.; Hopkins, C. R.; Niswender, C. M.; Rodriguez, A. L.; Venable, D. F.; Morrison, R. D.; Bubser, M.; Daniels, J. S.; Jones, C. K.; Conn, P. J.; Lindsley, C. W. Chemical modulation of mutant $mGlu_1$ receptors derived from deleterious *GRM1* mutations found in Schizophrenics. *ACS Chem. Bio.* **2014**, *9*, 2334−2346.
(13) Sheffler, D. J.; Wenthur, C. J.; Bruner, J. A.; Carrington, S. J. S.; Vinson, P. N.; Gogi, K. K.; Blobaum, A. L.; Morrison, R. D.; Vamos, M.; Crosford, N. D. P.; Stauffer, S. R.; Daniels, J. S.; Niswender, C. M.; Conn, P. J.; Lindsley, C. W. Development of a novel, CNS-penetrant, metabotropic glutamate receptor 3 ($mGlu_3$) NAM probe (ML289) derived from a closely related $mGlu_5$ PAM. *Bioorg. Med. Chem. Lett.* **2012**, *22*, 3921−3925.
(14) Bridges, T. M.; Rook, J. M.; Noetzel, M. J.; Morrison, R. D.; Zhou, Y.; Gogliotti, R. D.; Vinson, P. N.; Xiang, Z.; Jones, C. K.; Niswender, C. M.; Lindsley, C. W.; Stauffer, S. R.; Conn, P. J.; Daniels, J. S. Biotransformation of a Novel Positive Allosteric Modulator of Metabotropic Glutamate Receptor Subtype 5 Contributes to Seizure-Like Adverse Events in Rats Involving a Receptor Agonism-Dependent Mechanism. *Drug Metab. Dispos.* **2013**, *41*, 1703−1714.
(15) For information, see https://www.hepatochem.com/chemistry-screening-kits/bmo-kit/.
(16) See the Supporting Information for full details.
(17) Bunce, N. J.; McKinnon, H. S.; Schnurr, R. J.; Keum, S. R.; Buncel, E. Fragmentation pathways in the mass spectra of isomeric phenylazoxypyridine-N-oxides. *Can. J. Chem.* **1992**, *70*, 1028−1032.
(18) Sheng, W.-B.; Jiang, Q.; Luo, W.-P.; Guo, C.-C. Oxidative Rearrangement of Internal Alkynes To Give One-Carbon-Shorter Ketones via Manganese Porphyrins Catalysis. *J. Org. Chem.* **2013**, *78*, 5691−5693.
(19) Conn, P. J.; Lindsley, C. W.; Stauffer, S. R.; Zhou, Y.; Bartolome-Nebreda, J. M.; MacDonald, G. J.; Gogliotti, R. D.; Turlington, M. Substituted 5-(prop-1-yn-1-yl)picolinamide analogs as allosteric modulators of metabotropic glutamate receptor subtype 5. WO2013049255A1, 2013.
(20) Arienti, K. L.; Brunmark, A.; Axe, F. U.; McClure, K.; Lee, A.; Blevitt, J.; Neff, D. K.; Huang, L.; Crawford, S.; Pandit, C. R.; Karlsson, L.; Breitenbucher, J. G. Checkpoint Kinase Inhibitors: SAR and Radioprotective Properties of a Series of 2-Arylbenzimidazoles. *J. Med. Chem.* **2005**, *48*, 1873−1885.
(21) Srinivasan, N. S.; Lee Donald, G. Preparation of 1,2-diketones: oxidation of alkynes by potassium permanganate in aqueous acetone. *J. Org. Chem.* **1979**, *44*, 1574.

DOI: 10.1021/acsomega.9b02017
ACS Omega 2019, 4, 12782−12789